Variation of Friction Factor Through the Gait Cycle in an UHMWPE-CoCrMo Hip Endoprosthesis

FLORIN MUNTEANU*, PAUL BOTEZ
Orthopaedic Clinic, Clinical Hospital of Rehabilitation Iasi, Faculty of Medical Bioengineering, Iasi, 9-13 Kogalniceanu Str., 700454, Iasi, Romania

The frictional factor of new hip endoprosthesis was measured using one hip testing device designed in Biomechanics Laboratory of Medical Bioengineering Faculty. Hip simulator respect physiological condition (variable load, variable motion). The friction factor value for fluid film regime through the gait cycle was founded variable like a consequence of UHMWPE visco-elasto-plastic behaviour.

Keywords: *friction factor, gait cycle, visco-elasto-plastic behaviour*

John Charnley was the first who introduced low friction arthroplasty concept. In November 1962, he implanted a hip prosthesis using a high density polyethylene (HDPE) cup, which articulated with a stainless steel femoral head of 22,25 mm diameter. The principle of the low friction arthroplasty has remained the same ever since. Because HDPE have not a good wear resistance, ultra-high molecular weight polyethylene (UHMWPE) is introduced. Its molecular weight is approximately ten times that of HDPE. UHMWPE has highest impact strength of any plastic [1]. This biomaterial is choice for load-bearing articular components used in total joint arthroplasty, for prostheses of the hip, knee and elbow. It is highly resistant to wear and has low coefficient of friction. Under the articulation of artificial joints, UHMWPE acts as a bearing surface under the lubrication of synovial fluid containing various lipoproteins [2].

UHMWPE have a crystalline structure with a crystalline lamellae (10-50 μm length, 10-50 nm thickness placed at 10-50 nm distance), disposed in an amorphous matrix [3]. The degree of crystallinity C (lower than HDPE), of UHMWPE is known to strongly influence several of its tensile mechanical properties such as Young's modulus, yield stress and ultimate tensile properties. Young's modulus is proportional with C and yield stress with $(0,1 + C)^2$ [4].

There are two basic types of UHMWPE: standard and cross-linked (x-UHMWPE). Cross-linking of UHMWPE macromolecules has been performed using cross-linking agents such as peroxides, and through gamma or electron-beam irradiation. These process leads to a decreasing of crystalinity degree of UHMWPE and consecutively to decrease of Young modulus and yield stress, but this structure improve wear-resistance [4].

UHMWPE have a visco-elasto-plastic behaviour. A bidimensional impulse generation applied to polymers (like UHMWPE) show that the viscoelastic behaviour of polymers has consequence of impulse propagation [5]. Function of UHMWPE type (fabrication process), values of Young's modulus are: for UHMWPE E = 1,3÷1,7GPa and for x-UHMWPE E = 0,6÷1,1GPa [3, 6].

Plastic deformation of UHMWPE is occurring in: amorphous layers by interlamellar shear, interlamellar separation, lamella stack rotation, and in crystalline regions by chain slip, transverse slip and dislocation generation. Yield stress of UHMWPE is overcome between 20MPa and 24MPa [4].

Hip prosthesis includes a prosthetic nail that is implanted in femur, a femoral head, an acetabular cup (made by injection moulding [6]) that is inserted in coxal bone (fig. 1).

A great deal of studies, regarding the friction factor variation was performed in different testing conditions, like pin on disk, ball on plane, ball on socket, in dry regime or lubricated with different lubricants (distilled water, physiologic serum, plasma, etc.). The friction and wear behaviour of UHMWPE samples were studied by using ball sliding on UHMWPE disc under plasma lubrication and friction coefficient result in the lowest value around 0,075 [7]. In another study, the friction and wear properties of UHMWPE rubbing against the modified alloys under lubrication of distilled water were investigated using a pin-on-disc tribometer [8] where the value of friction coefficient was fond approximately 0,082. There are, also, studies who respect the physiological conditions where UHMWPE acetabular cups were tested against CoCrMo femoral heads in a hip joint simulator run for 2,5 million cycles in bovine calf serum [9].

No one of these studies established the friction factor variation for one gait cycle, complying to geometrical, loading and surface parameters. This variation being able to predict the medium value of the friction factor after the prosthesis was implanted in the femur.

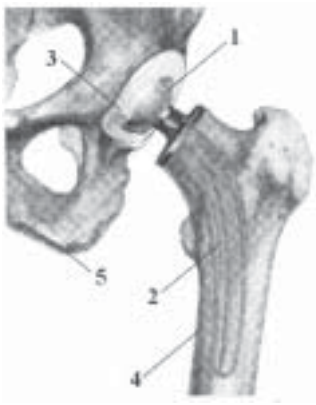

Fig. 1. Hip endoprosthesis: 1 – femoral head; 2 – prosthetic nail; 3 – acetabular cup; 4 – femur; 5 – coxal bone

* *email: florin.munteanu@bioinginerie.ro*

Considering these facts, a testing device was designed to determine tribological parameters for biomaterials used in hip prosthesis.

The device respects physiological conditions: variable loading with maximum load 2100 N; angular velocity similar to the one of flexion–extension movement for a hip joint. The materials used for this study are composed of CoCrMo alloy, which diameter is 32 mm, for the femoral head and UHMWPE for the acetabular cup, which diameter is 32,2 mm. These dimensions are the most used in orthopaedic clinics in last time. In order to get the friction factor variation for one gait cycle several phases must be fulfiled. First is theoretical calculation of friction moment, which combined with the angular velocity variation of the femoral head, would allow calculating the dissipated power corresponding to this moment; the second is focused to the measurement of the friction factor in time and the calculation of the dissipated power corresponding to the measured moment. Calculating the ratio between the two dissipated powers, the friction factor variation deducted for one gait cycle.

Theoretical formulation

Theoretical calculation of the power dissipated by friction for one gait cycle

By default, the power dissipated by friction expressed like this:

$$P_{DT} = M_{ft} \cdot \omega \qquad (1)$$

where:

P_{DT} – theoretical dissipated power;

M_{fT} – theoretical friction moment;

ω – angular velocity (variable) of the femoral head.

For theoretical calculation of the dissipated power, the moment represents, in this case, the friction moment corresponding to friction coupling femoral head – acetabular cup, and the angular velocity is the same one as in the flexion – extension motion.

Both loading and angular velocity were the ones gathered from the testing outfit, being the same ones for theoretical dissipated power and also for the experimental one.

Friction moment calculation

Let us consider the situation showed in figure 2, where the femoral head represented as a sphere, which ray is *r*, with the respect of a coordinate system *Oxyz*, where the point *O* is located in the centre of the sphere.

Flexion – extension motion (oscillator with an angular velocity ω) performed around the *Ox* axis, the maximum amplitude being 20° physiologically.

The resultant force *R* acted on the friction couple femoral head-acetabular cup, the result represented as a spherical calotte contact area.

Let us consider a point *A(x, y)* located inside the contact area, in which immediately neighbourhood was an elementary area *dx·dy*.

The distance *OA*, which was the sphere ray in fact, was making with the *xOy* the angle θ, and its projection, OA_1 was forming with *Ox* axis the angle ϕ.

The differential of friction moment calculated using the expression:

$$dM_{fT} = \mu \cdot dR \cdot A_1C \qquad (2)$$

where:

μ – friction factor;

R – the reduced force, which was acting on the femoral head (fig. 2);

A_1C – the perpendicular from point *A* on *xOy* plane.

- The arm force $A_1C \perp Ox_1$ (fig.1) was geometrically calculated and its value was founded:

$$A_1C = \rho \cdot \sin\phi \qquad (3)$$

where:$\rho = O_2A$, $\rho \in [0, a]$ with $a = O_1D$.

- The basic force *dR* could be expressed in relation with the stress:

$$dR = \sigma \cdot dx \cdot dy \qquad (4)$$

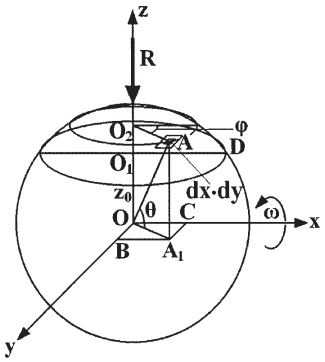

Fig. 2. The contact area between the femoral head and the acetabular cup

The next step was to consider the real situation when the sphere with radius *r*, was in contact with a viscous-elastic-plastic surface (fig. 3.a). Let us consider a new coordinate system $O_1x_1y_1z$, whose centre was located in the centre of the contact circle (projection of contact area). The equation of the sphere with the centre coordinates (0, 0,-z_0) is:

$$(x')^2 + (y')^2 + (z + z_0)^2 = r^2 \qquad (5)$$

and the equation of the surface contact circle, with radius *a* is:

$$(x')^2 + (y')^2 = r^2 - z_0^2 = a^2 \qquad (6)$$

Replacing z_0 from (6) in (5) it results:

$$z = \sqrt{r^2 - (x')^2 - (y')^2} - \sqrt{r^2 - a^2} \qquad (7)$$

If the relation (7) is differentiated with time *t* and (*dx'/dt)=V=*$\omega \cdot r$ (*V* representing the relative velocity of the sphere relative to the viscous-elastic plane), the result will be:

$$\dot{z} = \frac{x' \cdot V}{\sqrt{r^2 - (x')^2 - (y')^2}} \qquad (8)$$

A visco-elasto-plastic model is represented in figure 3.b, which is characterized by elasticity parameter *E*, the viscosity η and the equivalent flow stress σ_{ce}.

According to the third resistance theory [10]:

$$\sigma_{ce} = \sqrt{p_c^2 + 4 \cdot \tau_f^2} = \sqrt{p_c^2 \cdot (1 + 4 \cdot 0.5^2)} \qquad (9)$$

p_c = 22 MPa being the flow pressure of the softer material (in this case UHMWPE) [4], and τ_f the shielding stress of the same material, in conclusion: σ_{ce} = 31,112 MPa.

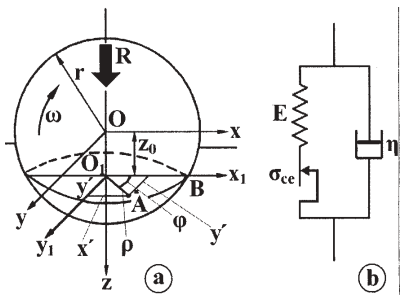

Fig. 3. The contact between rigid sphere and viscous-elastic-plastic plane: a) sphere-plane contact; b) viscous-elastic-plastic model

In figure 3b, the patina (corresponding to plastically deformation, defined by σ_{ce}) and the spring (corresponding to elastically deformation, defined by Young modulus *E*) is disposed in series, both being arranged in parallel with a viscous element (corresponding to dissipative element, defined by viscosity η). The model configuration is suggested by the successive deformation of plastic and elastic elements (function of load), both being concomitant with viscous deformation.

According to Prandtl-Reuss equations [10], the connection between stress and specific deformation (for plastically deformation) is:

$$\varepsilon = \frac{1-2\cdot\nu}{E}\cdot\sigma \tag{10}$$

where *n* - Poisson ratio.

On the other hand, according Saint-Venant principle [11], the connection between stress and specific deformation (for skate element) is:

$$\sigma = \sigma_c \cdot \frac{\dot{\varepsilon}}{|\dot{\varepsilon}|} \tag{11}$$

Since femoral head - acetabular cup contact is only in compression, $\sigma_{ce} = c \,.\, \sigma_c$, where $c \cong 3$ [12] is a contact geometry coefficient. By replacing the last equation in (10):

$$\varepsilon = \frac{1-2\cdot\nu}{E}\cdot\sigma_{ce} \tag{12}$$

viscous-elastic-plastic model is characterized by the next differential equation:

$$\sigma = E\cdot\varepsilon + \eta\cdot\dot{\varepsilon} + \sigma_{ce}\cdot(1-2\cdot\nu) \tag{13}$$

Considering $\varepsilon = z / L$[12], where *z* is defined by relation (7) and *L* is second typical length dimension [12]:

$$L = L^*\left(\frac{3\cdot N}{E'\cdot\sum\xi}\right)^{\frac{1}{3}} \text{ with } \sum\xi = \frac{1}{r_s}-\frac{1}{r_c}$$
$$\text{and } \frac{1}{E'} = \frac{1}{2}\left(\frac{1-\nu_s^2}{E_s}+\frac{1-\nu_c^2}{E_c}\right)$$

where:

r_s = 16mm femoral head radius;

r_c = 16.1mm internal acetabular cup radius;

E_s = 2.1. 10^2GPa femoral head (CoCrMo alloy) elasticity modulus;

ν_s = 0.3 femoral head Poisson coefficient;

E_c = 1,.4GPa acetabular cup (standard UHMWPE) Young modulus;

ν_c = 0.3 UHMWPE Poisson coefficient [4];

L* = 1 geometrical parameter [12].

Finally, the relationship between stress and *z* (7) is show by the next differential equation:

$$\sigma = E\cdot\frac{z}{L}+\eta\cdot\frac{\dot{z}}{L}+\sigma_{ce}\cdot(1-2\cdot\nu) \tag{14}$$

By replacing (7) and (8) in (14), stress expression for pure sliding contact, appears in the following form:

$$\sigma(x',y') = \frac{E_c}{L}\left[A-B+\frac{\eta\cdot\omega\cdot\delta}{E_c}+C\right]$$
$$\text{with } A=\sqrt{r^2-(x')^2-(y')^2}\,;\; B=\sqrt{r^2-a^2}\,;$$
$$\text{and } C=\frac{L\sigma_{ce}(1-2\nu_c)}{E_c} \tag{15}$$

Elementary force d*R*, can be written as:

$$dR = \sigma(x',y')\cdot dx'dy' \tag{16}$$

For an easier calculation on replace Cartesian coordinates with polar coordinates: x'=ρ . cosϕ and y' = ρ . sinϕ, ($\rho = \sqrt{(x')^2+(y')^2}\ \rho\in[0,a]$), so:

$$dR = \frac{E_c}{L}\left[C+\frac{\eta\cdot\omega}{E_c}\cdot\rho+D\right]\rho\cdot\sin\phi\, d\rho d\phi \tag{17}$$
$$\text{where } D=\sqrt{r^2-\rho^2}-\sqrt{r^2-a^2}$$

In the expression of the friction moment, the angular velocity will be considered with absolute value (the negative value of ω is not relevant for friction factor calculation).

The differential of friction moment calculated using the expression:

$$dM_{fT} = \frac{\mu E_c}{L}\left[C+\frac{\eta|\omega|}{E_c}\rho+D\right]\rho^2\sin\phi\, d\rho d\phi \tag{18}$$

By integer equation (18), result:

$$M_{fT} = 4\mu\int_0^a\int_0^{\frac{\pi}{2}}\frac{E_c}{L}\left[A+\frac{\eta\omega}{E_c}\rho+B\right]\rho^2\sin\phi\, d\rho d\phi =$$
$$= \mu\frac{E_c r^4}{L}\left[\sqrt{1-\frac{a^2}{r_s^2}}\left(\frac{a^3}{r_s^3}-\frac{a}{2r_s^2}\right)+\arcsin\left(\frac{a}{r_s}\right)\right]+$$
$$+\mu\frac{E_c r^4}{L}\left[\frac{\eta|\omega|}{4E_c}\frac{a^4}{r_s^4}-\frac{a^3}{3r_s^3}\left(\sqrt{1-\frac{a^2}{r_s^2}}-C\right)\right] \tag{19}$$

In previous expression, frictional moment has three components: elastic (M_{fTE}), viscous (M_{fTV}) and plastic (M_{fTP}):

$$M_{fT} = M_{fTE} + M_{fTV} + M_{fTP} \tag{20}$$

To distinguish the friction factor, (20) becomes:

$$M_{fT} = \mu\cdot(m_{fTE}+m_{fTV}+m_{fTp})$$

where:

$$m_{fTE} = \frac{E_c r^4}{L}\left[\sqrt{1-\frac{a^2}{r_s^2}}\left(\frac{a^3}{r_s^3}-\frac{a}{2r_s^2}\right)+\arcsin\left(\frac{a}{r_s}\right)\right]$$
$$m_{fTV} = \frac{E_c r^4}{L}\left[\frac{\eta\cdot|\omega|}{4E_c}\frac{a^4}{r_s^4}\right]$$
$$m_{fTP} = \frac{E_c r^4|\omega|}{L}\cdot\frac{a^3}{3r_s^3}\left(\sqrt{1-\frac{a^2}{r_s^2}}-\frac{L\sigma_{ce}(1-2\nu_c)}{E_c}\right)$$

The only parameter which is not known in the above expression was the ratio $\theta_f = \frac{\eta}{E_c}$, which represents the creeping time for UHMWPE, θ_f = 9400 s [13].

According to expression (1), the theoretical power dissipated by friction has three components: elastic (P_{DTE}), viscous (P_{DTV}), and plastic (P_{DTP}) defined by:

$$P_{DT} = P_{DTE}+P_{DTV}+P_{DTP} =$$
$$= |\omega|\cdot(M_{fTE}+M_{fTV}+M_{fTP}) =$$
$$= \mu\cdot|\omega|\cdot(m_{fTE}+m_{fTV}+m_{fTP}) = \tag{21}$$
$$= \mu\cdot(p_{fTE}+p_{fTV}+p_{fTP})$$

Experimental part

Describing the testing device designed for experimental determinations

The main aim of this paper was to measure the friction factor variation during one gait cycle and to show the factors that were important for this variation. Some consideration regarding the hip biomechanics show the

loading variation for one gait cycle (one step) and the principal movement of this joint flexion – extension. Considering this data, a testing device of the tribological parameters for the biomaterials used for hip endoprosthesis was designed, with an accurate respect of the biomechanics of the hip joint.

Considerations regarding the biomechanics of the hip joint
Dynamics elements

During gaiting, it is very difficult to estimate the action of the resultant force on the hip joint (fig. 4). The experimental measurements performed by Franek [14] with a dynamometric platform were leading to results, resumed by the equation curve:

$$\frac{R}{G} = \Phi\left(\frac{t}{\theta}\right) \quad (22)$$

R – reduced force which acts on the hip joint [N];
G – body weight without low limb weight [N];
θ – one step duration [s]; t – time [s].

The curves of the ratio between the reduced force R and the body weight variation during one-step are represented in figure 5.b. A similar variation was determined in [15].

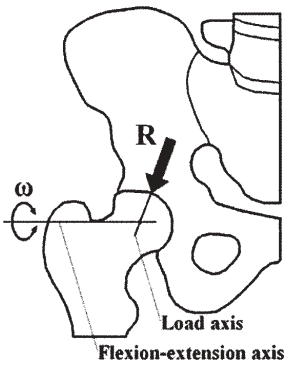

Fig. 4. Load axis and flexion extension axis at one hip joint

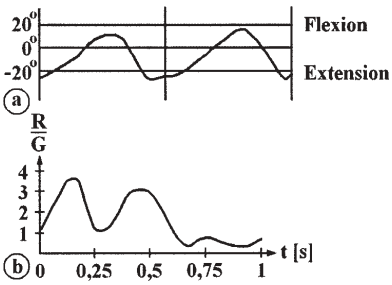

Fig. 5a.Variation of the flexion – extension during two gaits cycles; b - Variation of the ratio *F/G* during one normal gait cycle [14]

Kinematics elements

The hip joint is a typical spherical joint with three-movement axis. Therefore, it could perform three kind of movements: flexion-extension, abduction-adduction and internal-external rotation. The angular variation of the movements described above is presented in figure 5.a, during normal gait [14].

Cinematic scheme of testing device designed for friction experimental determination for hip endoprosthesis biomaterials

To materialize requirements of hip biomechanics, we made one testing device which scheme is depicted in figure 6.

The facilities of this device are the following: simultaneous or alternative measurements of friction coefficient and wear; perfect synchronization of kinematics and dynamics simulation of hip joint; respecting angle between load axis and oscillation axis. The device was built in such manner, that only the two spheres that oscillate in

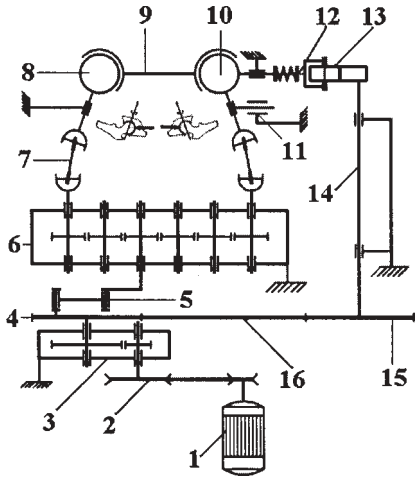

Fig. 6. Schematical representation of the testing device: 1 – electric engine; 2 – trapezoidal driving belts; 3 – reducing gear; 4 – leading chain wheel; 5 – quadrilateral gear; 6 – recurrent reducing gear; 7 – universal joint; 8, 10 – femoral head; 9 – double acetabular piece; 11 – beam; 12 – wedge gear; helical arc, 13 – cam; 14 – shaft; 15 – led chain wheel; 16 – rings and rolls chain

two directions, similar to the femoral head, sustained the acetabular piece (fig. 5, position 9).

The double acetabular piece is moving in the same time with the spheres because of the friction (fig. 6, positions 8 and 10). The measured friction moment is a projection of the real moment, the last one resulting from calculations. A mechanism cam - wedge - helical compression arc (fig. 6, position 12) achieved the specific loading for the hip joint; the cam (fig. 6, position 13) was synthesized corresponding with the loading diagram (fig. 5.b). The cam was geared in rotation by a chain driving (fig. 6, positions 4, 15, 16) and a shaft (fig. 6, position 14). The flexion-extension movement was described by a quadrilateral gear (fig. 6, position 5), which transformed the rotation of the chain wheel (figure 6, position 4) in to an oscillation.

This movement had a frequency of 1 Hz (achieved by reducing the angular velocity of the electric engine, position 1, by the trapezoidal driving belts, position 2, and the recurrent reducing gear, position 3). The oscillation was driven to femoral head by a cogwheels chain, its ratio being 1:1 (fig. 6, position 5) and a universal jointed coupling.

Experimental determination of the power dissipated by friction during one gait cycle

Dissipated power corresponding to one gait cycle, experimentally determined could be expressed as:

$$P_{DE} = M_{fE} \cdot \left|\omega_{pc}\right| \quad (23)$$

where:

P_{DE} - experimental dissipated power, corresponding to one gait cycle;
M_{fE} – experimental friction moment;
ω_{pc} – angular velocity (variable) of the acetabular piece, which was considered by default, positive on the entire duration of the gait cycle, the purpose being the acquiring a positive dissipated power, experimentally determined.

The measurement method of the friction factor was based on the displacement of the rigid lamella (position 5, fig. 7), which could deform the arc (position 4, fig.7). That led to an electrical tension variation by the displacement transducer (position 3, fig. 7), that would be assumed by the acquisition plaque of the computer.

It is notice that experiments were performed by using serum physiologic like lubricant.

The variation of the displacement is showed in figure 8.

The measured friction moment is:

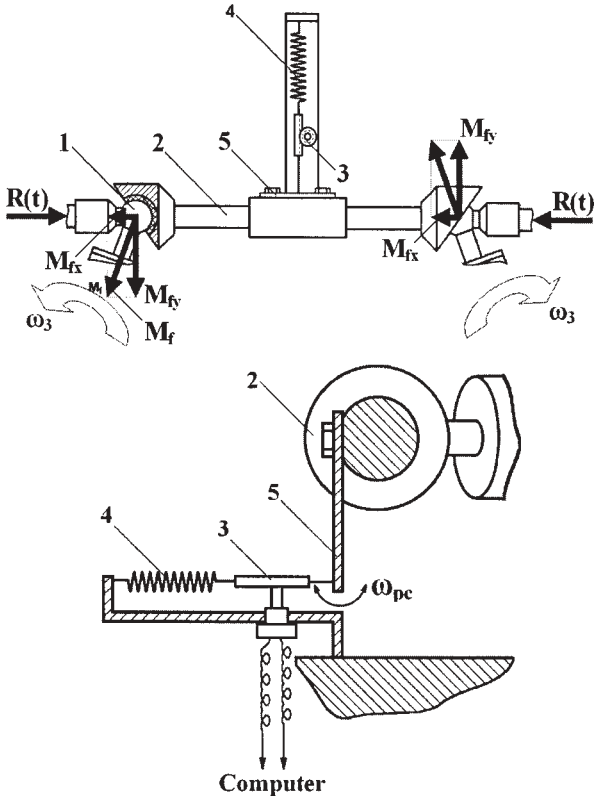

Fig. 7. Measurement method of the friction moment: 1 – femoral head; 2 – double acetabular piece; 3 – displacement transducer; 4 – helical traction arc; 5 – rigid lamella

$$M_{fm} = k \cdot x \cdot l \tag{24}$$

where:

k – elasticity parameter for the arc k = 14N/mm;

x – deformation of the arc, equal with the displacement of the lamella:

l – the length of the rigid lamella l = 63 mm.

The displacement of the rigid lamella - x - was determined experimentally, representing double of M_{fx} (fig. 7). The angle between the direction of R and the axis of the flexion - extension movement is 70°, the friction moment experimentally determined, M_{fx}, is:

$$M_{fE} = \frac{1}{2 \cdot \cos 70^o} \cdot M_{fm} = \frac{k \cdot x \cdot l}{2 \cdot \cos 70^o} \tag{25}$$

The experimental dissipated power is the scalar product between the friction moment and the angular velocity of the double acetabular piece ω_{pc}:

$$P_{DE} = \overline{M}_{fE} \cdot \overline{\omega}_{pc} = M_{fE} \cdot |\omega_{pc}| \cdot \cos 70^o \Rightarrow$$
$$P_{DE} = \frac{1}{2} \cdot k \cdot x \cdot l \cdot |\omega_{pc}| \tag{26}$$

The angular velocity of the double acetabular piece was expressed with the respect of the rigid lamella extremity v_l:

$$|\omega_{pc}| = \frac{|v_l|}{l} = \frac{1}{l} \cdot \frac{|\Delta x|}{\Delta t} \tag{27}$$

So, the expression of the experimental dissipated power is:

$$P_{DE} = \frac{k \cdot x}{2} \cdot \frac{|\Delta x|}{\Delta t} \tag{28}$$

Results and discussion

Experimental dissipated power must be equal with the theoretical one:

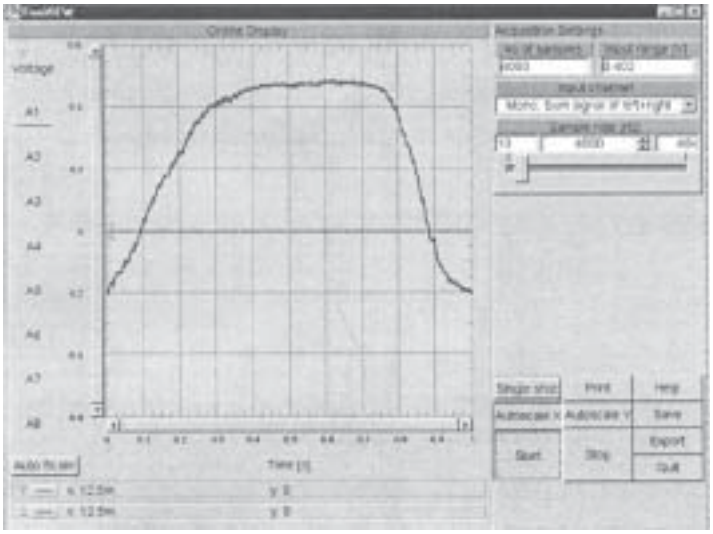

Fig. 8. Variation of the displacement x during a complete gait cycle

$$P_{DT} = P_{DE} \tag{29}$$

From the above equality was yielding the expression of the friction factor:

$$\mu = \frac{P_{DE}}{p_{fTE} + p_{fTV} + p_{fTP}} \tag{30}$$

$$\frac{1}{\mu} = \frac{p_{fTE} + p_{fTV} + p_{fTP}}{P_{DE}} = \frac{1}{\mu_E} + \frac{1}{\mu_V} + \frac{1}{\mu_P} \tag{31}$$

Where:

μ_E – elastic component of friction factor;

μ_V – hysteretic (viscous) component of friction factor;

μ_p – plastic component of friction factor.

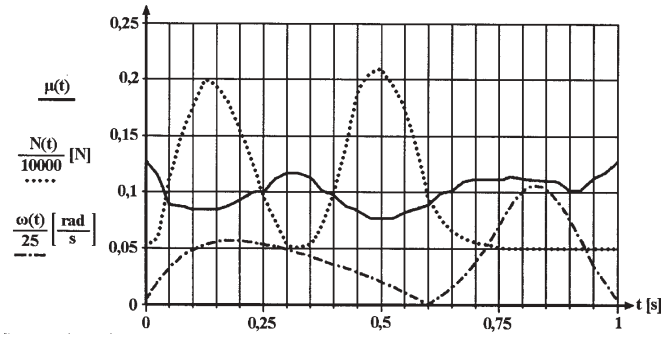

Fig. 9. Comparison between the friction factor, loading and the angular velocity modulus of the femoral head. It is to notice inverse dependency between the friction factor and load, and direct dependency with the angular velocity modulus

Variation of friction factor for a gait cycle is illustrated in figure 9. Maximum value of friction factor is 0.128 and minimum value is 0.077, so the average was 0.1025.

It is interesting to establish the relationship between the friction factor, loading and angular velocity. This comparison was represented in figure 9, where the loading was divided to 10^5, and the angular velocity modulus of the femoral head was divided to 50, in order to get the same range category. It is remarkable the inverse dependency with the charging variation and the direct dependency with the angular velocity modulus, for 75% of the time of one gait cycle.

For explaining this phenomenon, it is necessary a theoretical division of the friction factor, in its components: the UHMWPE roughness elastic and plastic deformation

component, and the hysteretic one (already determined in relation (31)).

Elastic deformation (proportional with the load increase), lead to a maximum roughness decreasing and by default to a decreasing of friction factor because the lubricating regime passes from boundary lubrication to thin-film lubrication; the last one is with a smallest coefficient of friction.

When roughness of UHMWPE surfaces increase (due to the abrasion of cement particles), the real pressure (who acts in the peaks of roughness) increases over the flow stress of UHMWPE.

In conclusion, the surface of the acetabular cup becomes smoother (in the contact area), that means plastic deformation of roughness peaks with the decrease of the roughness value. That induce too a thin film lubrication and a low value of friction coefficient.

In addition, when the angular velocity have a maximum value, the hysteretic friction increases too, and the total friction factor is bigger. This affirmation sustained by the diagram represented in figure 9 where the first minimum is bigger than the second.

Conclusions

After interpreting the theoretical and experimental results regarding the variation of the friction factor during one gait cycle, several conclusions would result:

- the friction factor is variable during one gait cycle;
- some increments could be assessed in the cases when the loading value is low and decrements where the loading value is high (fact that could be explained considering the roughness elasto-plastic deformation);
- because of the hysteretic component, the decrements were modelled by angular velocity, so that for a higher value of the angular velocity, a higher value of the first increment comparing to the second one was assessed (fig. 9);
- theoretical model of friction coefficient shows two components in boundary lubrication conditions:
  - elasto-plastic component which have a major significance;
  - hysteretic (viscous) component which have a minor significance due to high value of UHMWPE creeping time.

References

1.LEWIS, G., Biomaterials, 22, 2001 2001, p. 371
2.KURTZ et al. Biomaterials (20) 1998 p. 1449
3.BUTLER et al. Polymer (39): 1998, p. 39
4.BAJARIA S., BELLARE A., Medical Plastics and Biomaterials Magazine, on-line, March 1998
5.PUSCA S., PAUN MARIA-ALEXANDRA, TOMA C., Mat. Plast., 44, nr. 1, 2007, p. 39
6.FETECAU C., STAN FELICIA, Mat. Plast., 44, nr. 4,2007, p. 263
7.SHIBO W., SHIRONG G., Wear, 263, 7-12, p. 949
8.DANGSHENG X., ZHAN G., AND ZHONGMIN J., Surface and Coatings Technology, 201, 15, 2007, p. 6847
9.AFFATATO S., BERSAGLIA G., EMILIANI D., FOLTRAN I., TADDEI P., REGGIANI M., FERRIERI P., TONI A., Biomaterials, 24, 22, 2003, p. 4045
10.BUZDUGAN GH. Rezistenta materialelor Editura Tehnica Bucuresti, 1980
11.MALVERN L. E., Introduction of a Continuous Medium, Prentince Hall, 2001
12.TUDOR A., Contactul real al suprafeţelor de frecare, Editura Academiei, 1990
13.ABRAHAMS N., GOLDSMITH A. A., NICOL A. C., 12th Conference of the European Society of Biomechanics, Dublin, 2000, p. 226
14.FRANEK F, PAUSCHITZ A., KELMAN P., Proc. of 10th Int. Colloquim, Technische Akademie Esslingen, 1996, p. 1495
15.MEDVED V., Measurements of human locomotion, CRC Press, USA, 2000

Manuscript received: 18.12.2007